ACTA
AMAZONICA | http://dx.doi.org/10.1590/1809-4392202401751

BIODIVERSITY AND CONSERVATION | ORIGINAL ARTICLE

Microsternarchus javieri, a new species of weakly electric fish (Gymnotiformes: Hypopomidae, Microsternarchini) from the Negro River basin, Amazonas, Brazil

Carolina ESCAMILLA PINILLA[1*], Cristina COX FERNANDES[2,3], José Antônio ALVES-GOMES[4]

[1] Instituto Nacional de Pesquisas da Amazônia, Programa de Pós-Graduação em Biologia de Água Doce e Pesca do Interior, Manaus - Amazonas, Brasil

[2] University of Massachusetts, Morrill Science Center, Biology Department, Amherst -MA, 01003, USA

[3] Instituto Nacional de Pesquisas da Amazônia, PPG Biologia Aquática e Pesca Interior, C. P. 478, Manaus, Brazil

[4] Instituto Nacional de Pesquisas da Amazônia, Laboratório de Fisiologia Comportamental e Evolução, Manaus - Amazonas, Brasil

*Corresponding author: carolina.escamilla@inpa.gov.br

ABSTRACT

Here we describe a new hypopomid species, *Microsternarchus javieri* n. sp., encountered in flooded savanna streams of the Branco River and in *terra-firme* streams in the mid- and lower portions of the Negro River basin. We compared this new species with *M. bilineatus* from the San Bartolo River, Venezuela, and *M. brevis* from the upper portion of the Negro River. We also compared this new species with two recently described species in the genus *Microsternarchus, M. longicaudatus* and *M. schonmanni.* We examined morphometrics, anatomical characters, DNA barcode distances for the COI (cytochrome C oxidase subunit I) gene, and electric organ discharge (EOD) parameters. We diagnosed *M. javieri* n.sp. based on variation in maximum body depth, eye diameter, caudal vertebral counts, number of anal fin rays, and the shape of the maxillae. The average intra-specific genetic distance (K2P) in *M. javieri* n.sp. was 0.83%, whereas the average inter-specific genetic distance to *M. brevis* was 12.45%, and to other hypopomids ranged from 17.21 to 21.54%. When comparing EOD waveforms of the new species with *M. brevis*, we found differences in repetition rate, the ratio between the first and second phase areas, and the polarity balance. The description of *M. javieri* n. sp. increases to five the number of species in the genus.

KEYWORDS: fish taxonomy, biodiversity, DNA barcode, electric organ discharge, neotropical region.

Microsternarchus javieri, nova espécie de peixe elétrico (Gymnotiformes: Hypopomidae, Microsternarchini) da bacia do Rio Negro, Amazonas, Brasil

RESUMO

No presente estudo descrevemos uma nova espécie de hipopomídeo, *Microsternarchus javieri* n. sp., encontrada em riachos de savana da bacia do Rio Branco e em riachos de terra firme da bacia do baixo e médio Rio Negro. Comparamos esta nova espécie com *M. bilineatus* do Rio San Bartolo, Venezuela; e com *M. brevis* do alto Rio Negro. Comparamos também a nova espécie com duas espécies recentemente descritas do gênero *Microsternarchus, M. longicaudatus* e *M. schonmanni*. Examinamos a morfometria, caracteres anatômicos, distâncias genéticas no código de barras de DNA (gene COI - cytochrome C oxidase subunit I), e os parâmetros de descarga do órgão elétrico (DOE). Diagnosticamos *M. javieri* n. sp. com base na variação da altura máxima do corpo, diâmetro do olho, número de vértebras caudais, número de raios da nadadeira anal e formato da maxila. A distância média intra-específica (K2P) em *M. javieri* n. sp. foi 0.83%, enquanto que a distância média inter-específica com *M. brevis* foi de 12.45%, e outras espécies da família Hypopomidae variaram de 17.21 a 21.54%. Quando comparamos a forma da DOE da espécie nova com *M. brevis* encontramos diferenças na taxa de repetição, na razão da área da primeira fase sobre a segunda fase, e no equilíbrio de polaridade. Com a descrição de *M. javieri* n. sp., o número de espécies no gênero aumentou para cinco.

PALAVRAS-CHAVE: taxonomia de peixes, biodiversidade, código de barras DNA, descarga do órgão elétrico, região neotropical.

CITE AS: Pinilla, C.E. Fernandes, C.C. Alves-Gomes, J.A. 2025. *Microsternarchus javieri*, a new species of weakly electric fish (Gymnotiformes: Hypopomidae, Microsternarchini) from the Negro River basin, Amazonas, Brazil. Acta Amazonica 55: e55bc24175.

INTRODUCTION

The Negro River is the largest tributary of the left bank of the Amazon River, running along the southern frontier of Colombia and Venezuela, where it enters Brazil and, after 1200 km, meets the Solimões River to form the Amazon River (Alho et al. 2015). Throughout its path, the Negro River crosses distinct geomorphological units, including the ancient, magmatic Guiana Shield in its upper portion and the lowland sedimentary basin of the central Amazon River. Its black water is poor in mineral nutrients, yet it supports many fish species, 922 described so far, 90 of which are endemic (Dagosta and de Pinna 2019). In its lower and middle portions, the Negro River receives sediment-rich discharge from the Branco River and forms an area characterized by insufficiently drained floodplains that includes several patches of flooded savanna (Latrubesse and Franzinelli 2005; Junk et al. 2011; Moraes et al. 2021). The Branco River basin harbors 601 fish species, 23 of which are endemic (Dagosta and de Pinna 2019). Among the ichthyofauna of the Negro and Branco basins, the electric fishes (Order Gymnotiformes) are an important taxonomic component, forming a peculiar species assemblage that occupies microhabitats such as dead-sunk leaves, sandbanks, and roots.

The electric fish family Hypopomidae is a monophyletic group with six genera: *Akawaio, Brachyhypopomus, Hypopomus, Procerusternarchus, Racenisia* and *Microsternarchus* (Tagliacollo et al. 2016). The latter three genera comprise the tribe Microsternarchini (Albert 2001; Cox Fernandes et al. 2014). *Microsternarchus* can be distinguished from the other Microsternarchini genera by their long fine tail, lack of gill rakers, lack of scales in the middorsal region, distinct coloration patterns, and the visibility of the paired superficial dorsal rami of the posterior lateral line nerves, which appear as dark lines (Mago-Leccia 1994; Sullivan 1997; Cox Fernandes et al. 2015). At present, *Microsternarchus* comprises four species: *M. bilineatus* Fernández-Yépez 1968*, M. brevis* Cox Fernandes, Nogueira, Williston, Alves-Gomes 2015*, M. longuicaudatus* Sousa, Wosiacki, Muriel-Cunha, Prudente, Sousa, Peixoto 2024, and *M. schonmanni* Cox Fernandes, Keeffe, Escamilla Pinilla 2024.

For over two decades, JAG and collaborators have collected gymnotiforms in the floodplains, flooded savannas, and small streams of the Negro and Branco River basins. These surveys produced an extensive fish collection dominated by pulse-type gymnotiforms of the families Hypopomidae and Rhamphichthyidae. In the present study, we revisit the systematics of the tribe Microsternachini, for which a genetic analysis of mitochondrial DNA sequences of the cytochrome C oxidase subunit I (COI) gene revealed several distinct lineages in the Negro River (Maia and Alves Gomes 2012). We describe one of the lineages indicated by Maia and Alves Gomes (2012) (lineage C, from the mid and lower ranges of the Negro River) as a new species, comparing its morphometrics, anatomical characters, genetic sequences, and electric organ discharge (EOD) parameters to those of its congeners *M. bilineatus* and *M. brevis*.

MATERIAL AND METHODS

Specimen collection

From 2007 to 2022, many specimens were detected by JAG and collaborators with an electric fish finder and captured live with dip nets in small streams of the Negro and Branco River basins. Of these, 427 were assigned to lineage "*Microsternarchus* C" following molecular analysis by Maia and Alves-Gomes (2012). These fishes show all anatomical characters noted in the introduction for the tribe Microsternarchini. They originate from 47 collection points in *terra-firme* streams of the lower and mid portions of the Negro River, and the lower portion of the Branco River, georeferenced using QGIS (Develop Team 3.34 Geographic Information System SIRGAS 2000 datum).

Specimens used for morphometric and anatomical analysis are listed below in Material examined. Specimens used for molecular approaches are listed in the Supplementary Material (Table S1). Additional genetic sequences within the family Hypopomidae were obtained from the public database GenBank at the NCBI (https://www.ncbi.nlm.nih.gov/genbank/). Animal handling and euthanasia was approved by the commission on ethics in animal use at Instituto Nacional de Pesquisas da Amazônia (INPA) (CEUA 036/2012). Fish collection was authorized by Instituto Chico Mendes de Conservação da Biodiversidade (ICMBio) (SISBIO licenses # 14833-4, 14834-12). Specimens used here are deposited in the fish collections at Instituto Nacional de Pesquisas da Amazônia, Brazil (INPA), Academy of Natural Science of Drexel University, USA (ANSP), University of Massachusetts, Amherst, USA (MNHC), Illinois Natural History Survey (INHS), and Museum of Comparative Zoology at Harvard University (MCZ) (abbreviations follow Sabaj 2020).

Molecular data

We estimated the pairwise mitochondrial COI gene distances among all 427 specimens, corrected by the Kimura two-parameters model (K2P), and created a refined DNA matrix with 385 individuals whose average genetic distances were lower than 2.5%. From this DNA matrix, we selected 27 individuals representing the full range of geographical distribution and DNA diversity of the overall sample for further morphometric and genetic analyses (see Figure 1). We used the COI sequences of those 27 selected individuals to compose a second DNA/COI matrix that included 43 sequences of seven species as outgroup as follows: 26 sequences of *Microsternachus brevis*, three sequences of *Procerusternarchus pixuna* Cox Fernandes, Nogueira and Alves-Gomes, 2014,

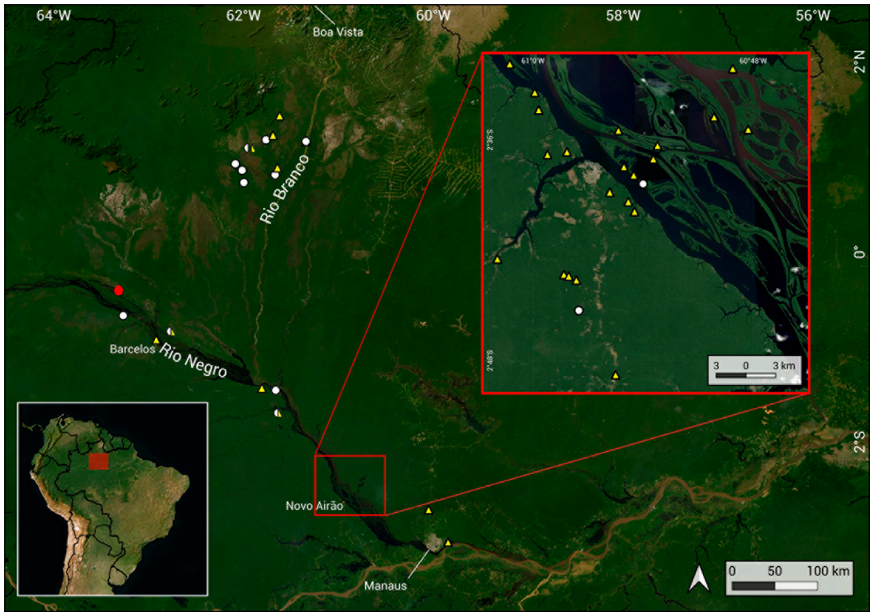

Figure 1. Geographical distribution of *Microsternarchus javieri* n. sp. specimens from 47 collection points (circles and triangles) along *terra firme* streams of the Branco River basin, Roraima state, and Negro River basin, Amazonas state, in Brazil. Type-locality indicated in red. White circles refer to the 15 location points of the specimens included in the morphological analysis. The inset (red rectangle) shows a closer view of the Anavilhanas Archipelago.

three sequences of *Racenisia fimbriipinna* Mago-Leccia, 1994, two sequences of *Akawaio penak* Maldonado-Ocampo, López-Fernández, Taphorn, Bernard, Crampton and Lovejoy, 2013, three sequences of *Brachyhypopomus brevirostris* Steindachner, 1868, three sequences of *Hypopomus artedi* Kaup, 1856, and three sequences of *Hypopygus neblinae* Mago-Leccia, 1994. This matrix contained COI sequences of all currently described genera of the Family Hypopomidae (see Supplementary Material, Table S1). Unfortunately, molecular data for *M. bilineatus* from Venezuela were not available for this analysis.

Anatomical data

The 27 individuals of the new species included 14 from *terra-firme* streams of the mid portion of the Negro River basin, three from the Anavilhanas Archipelago in the lower portion of the Negro River, all in Amazonas State, and 10 from small streams of the lower Branco River basin, Roraima state. We compared the new species with 14 individuals of *M. bilineatus* from San Bartolo River, Venezuela, and nine individuals of *M. brevis*, from the upper Negro River, Brazil (listed below in Comparative material examined). All morphometric measurements were taken by CCF using a dissecting microscope and a digital caliper to the nearest 0.1 mm. A total of 20 measurements were made, including total length (TL), length from snout to posterior end of anal fin (LEA), maximum body depth (D), distance from snout to anal-fin origin (SA), anal-fin base, from the first to last ray of anal fin (AF), head length, from tip of upper jaw to end of bony opercle (H), distance from snout tip to anterior edge of eye (S), mouth size as distance from tip of mandible to rictus (M), distance from snout to posterior edge of supraoccipital (SO), head depth at occiput (SV), snout to anterior edge of posterior naris (SN), eye diameter (ED), posterior edge of eye to opercle (EO), interorbital distance (IO), distance from anterior edge of eye to posterior border of posterior naris (NE), internarinal distance (ID), tip of snout to pectoral fin origin (SP), height of branchial opening from dorsal to ventral border (BO), caudal filament length from posterior end of anal fin to tip of caudal filament, (CL), and caudal filament depth at peduncle on the anterior part of the filament (CD). Specimens with damaged caudal filaments were excluded from the vertebral and anal fin counts and measurements.

Osteological nomenclature followed Hilton et al. (2007) and Cox Fernandes et al. (2014). Vertebral counts were made in 12 specimens, two using digital X-rays (settings were 51KV and 196 µA), and 10 cleared and double stained for cartilage and bone following a modified version of Dingerkus and Ulher (1977) where we used < 2 mg of trypsin in 30% sodium borate. Pre-caudal vertebral counts excluded the four elements of the Weberian complex, starting with the first centrum with a full neural spine and ending with the centrum before the displaced haemal spine. Caudal vertebrae counts began from the first vertebra associated with a haemal spine. Anal and pectoral-fin rays were the total number of branched and unbranched anterior rays. Pleural ribs and displaced haemal ribs were also counted. Scales above the lateral line near the mid-length of the body were counted to the dorsal midline. Sex was determined for six specimens by dissecting the abdominal cavity and examining the gonads under a

dissecting microscope. The head region of one specimen was CT-scanned using the MCZ on a Sky scan 1173 micro-CT with the following settings: 40 kV source voltage and 180 µA source current, and 7 urn voxel size. Isosurface models were generated and edited using Amira software. Tomographic models were generated with Mimics 16.0 for X64 (www.materialise.com). We followed Cox Fernandes et al. (2014, fig. 11, p. 107) for nerve terminology.

To identify and explore possible subgroups within our sample, we performed a principal component analysis (PCA) on the covariance matrix of 18 log-transformed morphometric measurements of 25 individuals of *M. javieri* n. sp. and 14 individuals of *M. bilineatus*. Two morphometric measurements, NE and BO, were highly variable across the dataset and two individuals had damage tails, these were removed from the PCA. Morphometric measurements with loadings > 0.3 in the first three principal components (PCs) were tested for homogeneity of slopes between species**.** When the interaction factor was not significant, a one-way analysis of covariance (ANCOVA) was performed while controlling for size differences among species. When the assumption of homogeneous slopes for the ANCOVA model was not met, the effect of the species was tested at ± 2 standard deviations around the mean of the covariate (size) (Logan 2010). All analyses were performed using RStudio (Version 4.3.1).

Electric organ discharge data

EODs were recorded for all individuals indicated as lineage C (N = 385) within a few hours after capture following the protocols outlined in Cox Fernandes et al. (2014). From those EOD recordings, 21 were excluded after a preliminary survey revealed that these fishes presented capture-related physical damage (shortened tail or other mechanical injury), which caused a significant distortion of the EOD waveform. Using Matlab® protocols, we obtained the average EOD for each recording, normalized to 5V peak-to-peak amplitude. To obtain the average EOD for the entire sample, the EODs obtained for all recordings were aligned to the peak of the first positive phase. We followed the traditional idea that zero-crossings of the signal delimit a phase (Heiligenberg and Rose 1985a,b). Additional parameters are shown in the Supplementary Material (Table S3). We then analyzed and compared EOD parameters of all 364 individuals indicated as lineage C against the 27 individuals selected for the morphometric comparisons to check if the subsample retained an accurate representation of the larger group (see Supplementary Material, Table S4). Moreover, we compared EODs between individuals with maturational stages ≥ 3 according to Leino et al. (2005) to further assess sexual dimorphism in the EODs (N = 44 females, N = 11 males). Finally, we compared the EOD waveform of the subsample against the EOD waveform of *M. brevis* individuals (N =16) used in Cox Fernandes et al. (2015) testing the most significantly different EOD parameters through a two-sample t-test. EOD recordings for *M. bilineatus* were not available for comparison.

RESULTS

***Microsternarchus javieri,* sp. nov.** Cox Fernandes, Escamilla Pinilla, Alves-Gomes

ZooBank registration: urn:lsid:zoobank.org:pub:8ACF274D-993E-49B8-ACCA-35F534050888

Figures 2 to 5, Table 1

Microsternarchus cf. bilineatus (Nogueira 2011)

Microsternarchus cf. bilineatus (Linhagem C-1, C-2) (Maia and Alves-Gomes 2012)

Microsternarchus bilineatus (Jesus et al. 2016)

Holotype: adult male of 98.6 mm TL (INPA-ICT 060886, 98.6 mm TL, adult male.). The type locality is Igarapé Aduiá, 0°24’17.8”S, 63°18’51.6”W, Negro River basin, 145 km upstream from the city of Novo Airão, Amazonas state, Brazil. Collected by Alves-Gomes and collaborators on January 14, 2007.

Paratypes: BRAZIL. Amazonas, Negro River basin: same data as holotype, INPA-ICT 060867, 1 male, 93.7 mm TL EOD 0701141336E-ADU053, INPA-ICT 28591, 2, 98.8 mm TL EOD 0701141336E-ADU052, and 81.9 mm TL EOD0701141336E-ADU045; Igarapé Cajurí 1°41'42.7"S, 61°38'7.4"W, INPA-ICT 42261, 1 female, 99.1 mm TL EOD 0503131015D-CAJ0013; Igarapé Quimicurí 0°40'14.9"S, 63°16'3.6"W, INPA-ICT 060868, 67.5 mm LEA EOD 0701141250D-QUI015; Ilha Novo Airão 2°38'23.2"S, 60°53’59.9”W, ANSP 212283, 3, 1 male, 101.2 mm TL EOD 0802191600I-NAI01, 88.4 mm TL EOD 0802191600I-NAI009, and 95.0 mm TL EOD 0802191600I-NAI002; Igarapé Moura 1°27’23.07”S, 61°39’38.2”W, ANSP 212284, 85.8 mm TL EOD 0802200000D-MOU005. Roraima, Branco River basin: Igarapé Agua Boazinha 1°9'41.6"N, 61°20'30.2"W, ANSP 212289, 91.4 mm TL EOD 1112091430D — ABZ015, INPA-ICT 060873, 85.1 mm TL EOD 1112091430D-ABZ_020, INPA-ICT 060874, 78.3 mm TL EOD 1211061050D-ABZ035; Catrimani River: Igarapé Arapixi 0°55'33.61"N, 62°5'9.58"W, ANSP 212290, 2, 99.9 mm TL EOD 1211111534D-AXI0012 and 103.4 mm TL EOD 1211111534D-AXI0029, INPA-ICT 060877, 3, 57.6 mm LEA EOD 1211111534D-AXI01, 85.4 mm TL EOD 1211111534D-AXI04, and 59.8 mm LEA EOD 1211111534D-AXI031; Igarapé Caixa 0°51’29.7”N, 62°0’53.22”W, ANSP 212285, 85.4 mm TL EOD 1211120800E-CAX0018, INPA-ICT 060869, 2, 76.5 mm TL EOD 1211120800E-CAX020, and 83.7 mm TL EOD 1211120800E-CAX030; Igarapé Camoji 0°43'44.1"N, 69°59'44.6"W, ANSP 212286, 95.5 mm TL

EOD 1211121216D-OJI020, INPA-ICT 060870, 2, 54.9 mm LEA EOD 1211121216D-OJI023, and 74.2 mm TL EOD 1211121216D-OJI029; Agua Boa do Univini River: Igarapé Bacaba 1°10'40.8"N, 61°45'48.2"W, ANSP 212288, 75.8 mm TL EOD 1112071540D-BAC08, INPA-ICT 060872, 2, 54.2 mm LEA EOD 1112071540D-BAC09 and 56.3 mm LEA EOD 1112071540D-BAC010; Igarapé Preto 1°5'37.9"N, 61°56'58.1"W, ANSP 212291, 84.1 mm TL EOD 1112081150D-PRT0036; Igarapé Campo 0°48'38.9"N, 61°39'58.1"W, ANSP 212287, 2, 84.6 mm TL EOD 1211071610D-CAM07, and 91.8 mm TL EOD 1211071610D-CAM010, INPA-ICT 060871, 81.7 mm TL EOD 1211071610D-CAM08; Igarapé Extremo 1°25'54.2"N, 61°37'9.2"W, INPA-ICT 060876, 2, 75.9 mm LEA EOD 1211081354D-EXT02, and 79.8 mm TL EOD 1211081354D-EXT09. Collected by Alves-Gomes and collaborators.

Non-types: BRAZIL. Amazonas, Negro River basin: Igarapé Aduiá 0°24'17.8"S, 63°18'51.6"W, INPA-ICT 28591, 2 (C+S) 90.3 mm TL EOD 0701141336E-ADU042, and 86.9 mm TL EOD 0701141336E-ADU047; Igarapé Tapurú 2°45'16.6"S, 60°57'30.1"W, UMA F21050, 103.2 mm TL EOD 2004161000D-TPR04, UMA F21051, 111.7 mm TL EOD 2004161000D-TPR06, UMA F21052, 97.1 mm TL EOD 2011261430D-TPR05. Roraima: Branco River basin: Igarapé Água Boazinha 1°9'41.6"N, 61°20'30.2"W, INPA-ICT 060874, 69.9 mm TL EOD 1211061050D-ABZ050; Catrimani River: Igarapé Arapixi 0°55'33.61"N, 62°5'9.58"W, INPA-ICT 060877, 82.4 mm TL EOD 1211111534D-AXI020; Igarapé Caixa, 0°51'29.7"N, 62°0'53.22"W, INPA-ICT 060869, 78.6 mm TL EOD 1211120800E-CAX011; Igarapé Camoji 0°43'44.1"N, 69°59'44.6"W, INPA-ICT 060870, 67.3 mm TL EOD 1211121216D-OJI030; Água Boa do Univini River: Igarapé Extremo 1°25'54.2"N, 61°37'9.2"W, INPA-ICT 060876, 66.8 mm TL EOD 1211081354D-EXT03; Igarapé Escondido, 1°13'33.91"N, 61°41'21.87"W, INPA-ICT 060875, 73.9 mm TL EOD 1211091253D-ESC016. Collected by Alves-Gomes and collaborators.

Table 1. Morphometric data of holotype (INPA-ICT 060886) and paratypes of *Microsternarchus javieri* n. sp. TL = Total length. LEA = Length to end of anal fin. HL = Head length. N = sample size. SD = standard deviation.

Character	Holotype	Range	Mean	SD	N
Total length (mm)	98.6	74.5 – 111.7	93.2	9.0	25
Length to end of anal fin (mm)	67.5	54.2 – 73.9	63.9	4.8	25
Head length to bony opercle end (mm)	8.1	5.7 – 9.0	8.1	0.7	25
Caudal filament length (%TL)	32.6	26 – 44	32.6	3.3	25
Maximum body depth/ LEA	6.1	8 – 10	9.3	0.7	25
Snout to anal-fin origin/ LEA	21.2	19 – 26	23.1	1.7	25
Anal-fin length/ LEA	79.7	73 – 82	77.2	2.0	25
Head length to bony opercle end/ LEA	11.9	10 – 13	12.7	0.7	25
Snout length to supraoccipital/ LEA	10.3	9 – 12	10.7	0.6	25
Snout length to pectoral fin origin/ LEA	13.4	12 – 15	13.6	0.7	25
Depth of caudal filament at peduncle/ LEA	1.3	1.1 – 1.6	1.4	0.2	25
Snout to eye/ HL	31.7	23 – 36	29.1	2.3	25
Mouth from snout tip to rictus/ HL	19.1	18 – 26	21.3	2.1	25
Head depth at occiput/ HL	64.6	58 – 73	64.3	3.8	25
Snout length to posterior naris/ HL	21.9	20 – 30	24.5	2.5	25
Eye diameter/ HL	13.5	10 – 15	12.8	1.1	25
Eye to opercle/ HL	59.2	53 – 68	59.1	3.6	25
Eye to posterior naris/ HL	3.3	20 – 30	24.5	2.5	25
Interorbital distance/ HL	25.0	19 – 32	22.9	2.6	25
Internarinal distance/ HL	20.8	13 – 27	21.9	3.5	25
Branchial opening/ HL	29.6	17 – 36	24.3	4.7	25

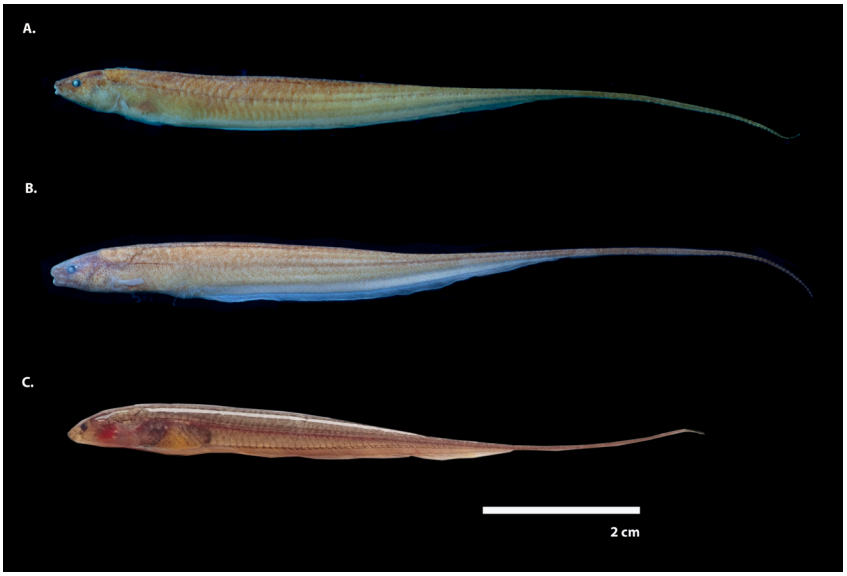

Figure 2. Lateral view of *Microsternarchus javieri* n. sp. from the Negro River basin. **A** – Holotype (INPA-ICT 060886), 98.6 mm TL, 67.6 mm LEA; **B** – Paratype (ANSP 212283), 101.2 mm TL, 62.0 mm LEA; **C** –Non-type (INPA-ICT 28591), 86.9 mm TL, 60.4 mm LEA live specimen.

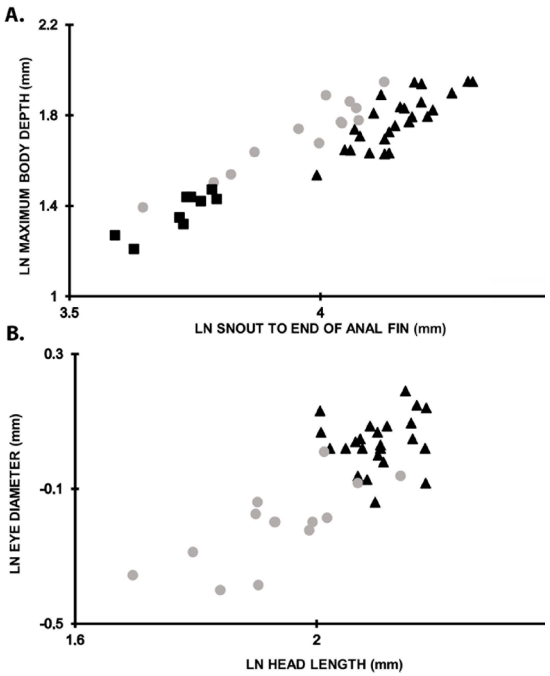

Figure 3. Relationship between length of snout to end of anal fin vs maximum body depth ($F_{2,43} = 19.41$, $p < 0.0001$) (**A**) and head length vs eye diameter ($F_{1,35} = 12.17$, $p = 0.001$) (**B**) in *Microsternarchus javieri* n. sp. (black triangles), *M. bilineatus* (grey circles) and *M. brevis* (black squares) individuals. A one-way analysis of covariance (ANCOVA) was performed while controlling for size differences among species. The data were log-transformed (LN).

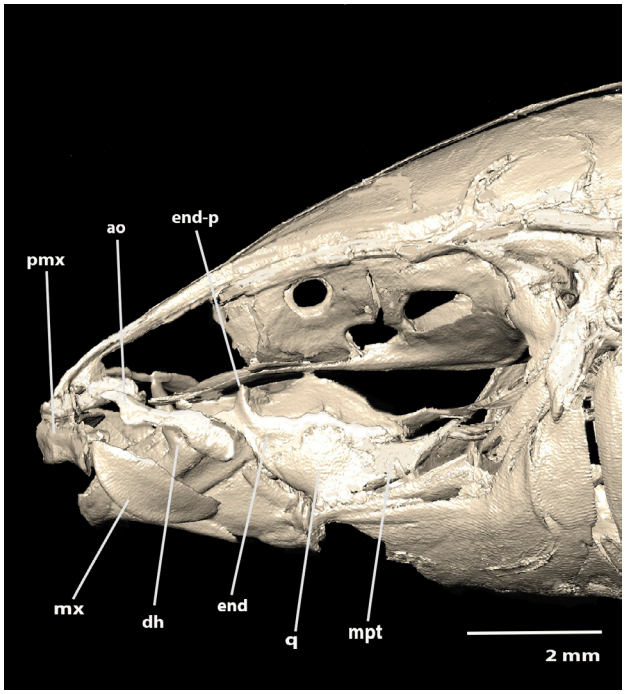

Figure 4. CT scan image of model head skeleton in lateral view of *Microsternarchus javieri* n. sp. (specimen INPA-ICT 060868, approx. 99.2 mm TL, 67.5 mm LEA). Abbreviations: ao = antorbital; dh = dentary hook; end = endopterygoid; end-p = endopterygoid process; mx = maxilla; mpt = metapterygoid; pmx = pre-maxilla; q = quadrate.

Diagnosis: *Microsternarchus javieri* n. sp. is distinguished from its congeners in having a smaller maximum body depth [8 – 10% of LEA, vs. in *M. bilineatus* 9.8 – 12% of LEA; in *M. brevis* 8 – 11.2% of LEA (Figure 3a), *M. longicaudatus* 7.9 – 11.5% of LEA and *M. schonmanni* 8.2 – 11% of LEA]. *M. javieri* n. sp. is further distinguished from *M. bilineatus* by a combination of characters: slightly larger eye diameter (10 – 15% of HL, vs. 10.1 – 13.5% of HL, Figure 3b), longer caudal filament (26 – 44% of TL vs. 29.3 – 34.4% of TL), fewer caudal vertebrae 60 – 65 (N = 11) vs. 66 – 67 (N = 3),

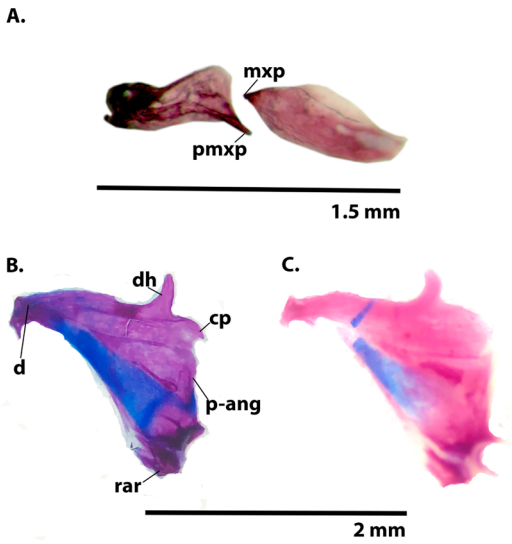

Figure 5. Osteological elements of the head of *Microsternarchus javieri* n. sp. (cleared and stained). **A** – Right side medial view of premaxilla and maxilla (58.8 mm TL, 43.0 mm LEA); **B** – Left side external view of dentary bones of immature specimen (62.9 mm TL, 45.6 mm LEA); **C** – Adult specimen (101.6 mm TL, 66.9 mm LEA). Abbreviations: cp = coronoid process; d = dentary bone; dh = dentary hook; mxp = maxilla process; p-ang = ascending process of anguloarticular; pmxp = premaxilla process; rar = retroarticular.

greater number of anal fin rays 146 – 174 vs. 138 – 161. *M. javieri* n. sp. is also distinguished from *M. brevis* by a much longer caudal filament (26 – 44% of TL vs. 12.8 – 20.9% of TL) and total length (74.5 – 111.7 mm vs. 37.5 – 53.2 mm), a greater number of caudal vertebrae [60 – 65 (N = 11) vs. 40 – 55 (N = 8)], and a greater number of anal fin rays (146 – 174 vs. 124 – 151). Compared to *M. longicaudatus*, *M. javieri* n. sp. has a larger eye diameter (10 – 15% of HL vs. 6.2 – 10.4% of HL) and fewer displaced haemal spines (2 – 3 vs. 3 – 4). *M. javieri* n. sp. can be further distinguished from *M. schonmanni* by a slightly longer caudal filament (26 – 44% of TL vs. 32.1 – 38.7% of TL) and fewer anal fin rays (146 – 174 vs. 164 – 192). The ventral margin of the maxilla of *M. javieri* n. sp. has a convex shape in adults and less convex to straight in juveniles (Figures 4, 5a). In *M. bilineatus* this margin is only partially convex, less curved, and tends to narrow posteriorly (see Fig. 4a and 6 in Cox Fernandes and Williston 2017); in *M. brevis* (see Fig. 4a in Cox Fernandes et al. 2015) and in *M. longicaudatus* this margin is not convex (see Fig. 2 in Sousa et al. 2024). The maxilla in *M. brevis* is larger than in *M. javieri* n. sp. (using the antorbital as a reference).

Description: Measurements and proportions of *Microsternarchus javieri* n. sp. are summarized in Table 1. Head, body shape, and pigmentation are illustrated in Figure 2 and 6. Body small**,** TL = 74.5 – 111.7 mm, LEA = 54.2 – 73.9 mm, body elongated and laterally compressed with dorsal profile slightly convex and ventral profile straight. Maximum body depth taken along the abdominal region**,** 8 – 10% of LEA. Body covered with cycloid scales, except on the head and anteriorly on the nape. Lateral line is complete**,** with large pores in head region. Lateral ramus of posterior lateral line nerve (LRPLLN) dark and clearly visible in most specimens. Dorsal ramus of posterior lateral line nerve (DRPLLN) dark and visible mainly in anterior portion closest to posterior lateral line nerve (PLLN). Dorsal and ventral segmental lateral line rami sometimes dark and visible (see Fig. 11 in Cox Fernandes et al. 2014, p. 107). Five to six scales above and six to seven below lateral line posterior to end of pectoral fin. No caudal or dorsal fins. Anal fin elongated and positioned posteriorly (73 – 82% of LEA), caudal filament (26 – 44% of TL), and relatively shallow (1.1 – 1.6% of LEA). Head laterally compressed and lightly convex from snout to occiput with length 5.7 – 9.0 mm and depth at occiput 58 – 73% of HL. Mouth slightly inferior in length, 18 – 26% of HL from snout to rictus (Figure 2). Moderately small snout 23 – 36% of HL. Internarinal distance 13 – 27% of HL, with both nostrils circular and posterior nares close to eyes. Large eye diameter of 10 – 15% of HL, positioned laterally, subcutaneously, and at mid-horizontal line.

Osteological remarks: Upper and lower jaws lack teeth. A well-developed posteroventral bony process of premaxilla (Figure 4 and 5a). Anterodorsal face of maxilla straight. Posteroventral margin of maxilla convex, with a half-oval shape (Figure 5a). Dentary margin almost straight in lateral view, its posterodorsal margin continuing posterior to a hook-like process or dentary hook, ending in coronoid process (Figure 5b, c). The dentary hook process is conical, vertical to slightly curved, with the tip pointing anteriorly (Figure 5b,c). The juvenile C+S specimen exhibits a more evident Meckel´s cartilage (Figure 5b) when compared to the adult (Figure 5c). Endopterygoid positioned dorsomedially to lower jaw, dorsal process of endopterygoid conical and vertical, and its tip narrow and short (Figure 4). Abdominal cavity with 11 – 14 pleural ribs (N = 13) and 2 – 3 displaced haemal spines in its posteroventral wall (N = 6). Precaudal vertebrae counts 12 – 14 (N = 12) and caudal vertebrae counts 60 – 65 (N = 11). Gas bladder ovoid-like anteriorly and long, balloon-like posteriorly with a transparent whitish color. Anal fin with 146 – 174 branched rays (N = 22). Pectoral fin hyaline, slightly round and short with 10 – 12 fin rays (N = 22).

Coloration in life (Figure 2c): Overall coloration yelllow to light brown. Denser concentration of chromatophores along dorsal surface of body and caudal filament, when compared to a lighter and more translucent appearance of ventral surface. Infraorbital, mandibular, and preopercular sensory canals sometimes visible. DRPLLN usually visible and dark. Gas bladder, liver, and vertebral column sometimes visible. Anal fin hyaline with posterior rays pigmented with several chromatophores at the base of pterygiophores. Pectoral fin hyaline. In lighter specimens, the electric organ above anal fin sometimes visible and transparent.

Coloration in alcohol: Coloration patterns varied among individuals of *Microsternarchus javieri* n. sp. Some have a mottled pattern with patches above the lateral line along the body (Figure 2 a and b) and others have a plain body without them (Figure 6c). The presence of high-density chromatophores also vary among individuals, for example, in the dorsal surface of the head, snout, and the area posterior to the pectoral fin (6a, b and c)."

Distribution and habitat: *M. javieri* n. sp. was collected in *terra firme* streams in the Negro River basin up to the municipality of Santa Isabel, Amazonas state, Brazil, and in flooded shield savannas in the Branco River basin, Roraima state, Brazil (Figure 1). These fish inhabit well-oxygenated streams with slow currents, and are thus not present in the main river channel. During the day, when at rest, they have a microhabitat preference for shallow areas of 0.3 to 1.5 m depth in the dry season, with a great abundance of dead leaves, abundant roots, leaf litter, vegetation cover, and tangled roots. JAG measured a water temperature of 26.1 – 29.7°C, pH 4.41 – 5.58, water conductivity of 9 – 37 µS cm^{-1}, and dissolved oxygen 3.02 – 6.3 mg L^{-1}. JAG noted when capturing these fish, that they usually occur in sympatry with other gymnotiform species such as *Brachypopomus, Hypopygus*, *Racenisia*, *Gymnorhamphichthys*, *Steatogenys* and *Electrophorus*.

Etymology: The specific epithet, *javieri*, is in honor of the late Javier Maldonado Ocampo, whose research on gymnotiforms, systematics, and conservation greatly contributed to our understanding of the Neotropical ichthyofauna. A masculine noun in apposition.

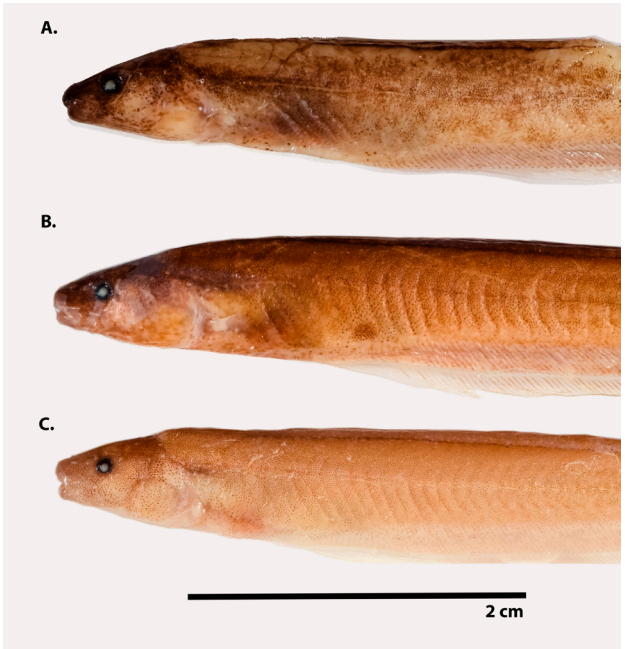

Figure 6. Right side lateral view of three specimens of *Microsternarchus javieri* n. sp. showing the differences in pigmentation. **A** – UMA F21051, 111.77 mm TL; **B** – ANSP 212290, 103.4 mm TL (paratype); **C** – INPA-ICT 28591, 74.5 mm TL (paratype).

Electric organ and EODs: The electric organ of *M. javieri* n. sp. occupies approximately 6% of the maximum body depth and 54% of the length from the snout to the posterior end of the anal fin. The electric organ is found in the posterior two thirds of the body above the proximal anal-fin radials, more visible in lighter individuals over the last third of the body. It is not visible, however, in the caudal peduncle. No accessory electric organ was found in the head or humeral region. The average EOD waveform had three phases of alternating polarity (Figure 7a). The third EOD phase was absent in specimens with broken or damaged caudal filaments (Cox Fernandes et al. 2015).

We observed sexual dimorphism in the discharges (Figure 7b). At rest, mature males had a slower repetition rate (87.07 ± 12.76 Hz) than females (100.45 ± 11.40 Hz), and their average peak power frequency was slightly lower (0.39 ± 0.06 KHz) than in females (0.46 ± 0.04 KHz). Interestingly, the most conspicuous difference between the two discharges was the expansion of the second (negative) phase in males, a generalized phenomenon among pulse-type gymnotiforms (Hopkins et al. 1990). The polarity balance was -9.42 ± 11.64 % in females and -23.53 ± 10.99 % in males, whereas the relative area of the second phase was -54.71 ± 5.82 and -61.76 ± 5.94, respectively.

In comparison with *M. brevis*, the EOD waveform of *M. javieri* n. sp. had a higher repetition rate (t-test, $t = -4.069$, $df = 37.76$, $p < 0.001$), a higher polarity balance (t-test, $t = 5.815$, $df = 39.78$, $p < 0.001$), a smaller first phase area (t-test, $t = 4.25$, $df = 31.67$, $p < 0.001$), but a greater second phase area (t-test, $t = 5.815$, $df = 39.78$, $p < 0.001$), and thus a greater ratio between the second and first phases (t-test, $t = -5.506$, $df = 39.97$, $p < 0.001$) (Figure 7c; Supplementary Material, Table S3).

The molecular analysis revealed that, while all the pairwise K2P intra-clade distances were smaller than 1%, the distance between the *Microsternarchus* species was above 12% (Table 2). To the other hypopomids and the outgroup, genetic distances ranged between 17% and 24%. The intra-clade pairwise distance for the DNA matrix with the 385 individuals of *M. javieri* n. sp. ranged from 0% to 2.45%, whereas for the 27 selected individuals it ranged from 0% to 2.18%.

The PCA analysis of external morphology variables indicated no significant difference among specimens from the Negro and Branco River basins, and no significant subgroups were revealed. PC1 explained 81% of the total variance, PC2 4.4%, and PC3 3%. The morphological measurements with loadings > 0.3 were ED and SN in PC2 plus CD, IO, ID, and D in PC3 (Supplementary Material, Table S2). Interaction among the six measurements was not significant, therefore all

variables were included in the ANCOVA (Table 3). There were significant differences among the three species in D with LEA as covariate ($F_{2,43}$ = 19.41, p << 0.001) (Figure 3a) and between *M. javieri* n. sp. and *M. bilineatus* in ED with H as covariate ($F_{1,35}$ = 12.17, p = 0.001) (Figure 3b).

DISCUSSION

Our combined genetic and comparative morphological evidence support the description of *Microsternarchus javieri* n. sp., previously noted by Maia and Alves-Gomes (2012) as *Microsternarchus* lineage C. The 27 specimens of the

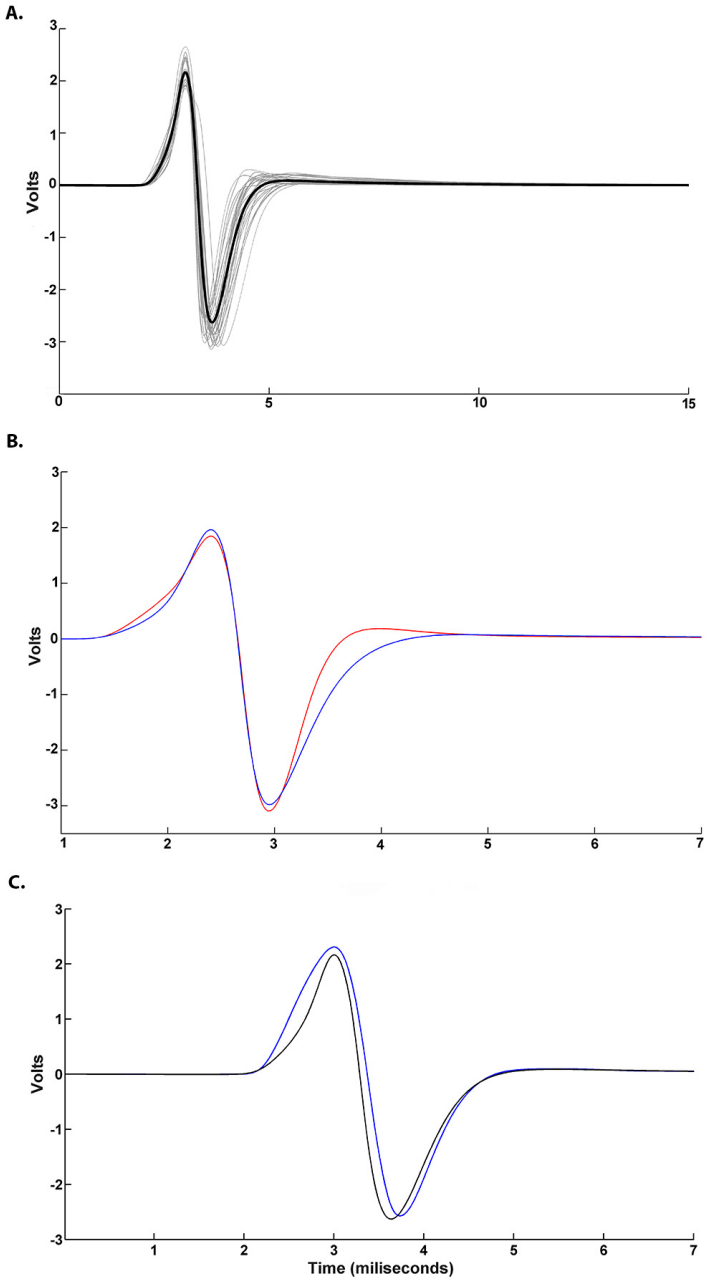

Figure 7. Electric organ discharge (EOD) waveform of *Microsternarchus javieri* n. sp. from *terra firme* streams of the Negro and Branco River basins, Brazil, recorded at rest. **A** –Average EOD waveform (in black), all other EOD waveforms in grey (N = 27); **B** – Average EOD waveform of females (in red) (N = 44) and males (in blue) (N = 11); **C** – Average EOD waveforms of *M. javieri* n. sp. (in black) (N = 27) compared with *M. brevis* (in blue) (N = 15).

Table 2. Average pairwise Kimura two-parameters model (K2P) genetic distances (%) within species (diagonal, in bold) and between the seven hypopomid species and the outgroup (see details in Supplementary Material, Table S1).

Species	H. nebli	A. penak	H. arted	B. brevi	R. fimbr	P. pixun	M. javie	M. brevi
Hypopygus neblinae	**0.26**							
Akawaio penak	21.39	**0.48**						
Hypopomus artedi	21.57	20.19	**0.26**					
Brachyhypopomus brevirostris	23.19	19.43	19.99	**0.47**				
Racenisia fimbriipinna	20.08	21.51	20.48	19.79	**0.40**			
Procerosternarchus pixuna	20.77	20.83	20.16	21.12	19.12	**0.47**		
Microsternarchus javieri n. sp.	21.54	21.36	20.00	20.16	18.17	17.21	**0.83**	
Microsternarchus brevis	23.28	22.28	22.45	19.87	17.97	17.40	12.45	**0.63**

Table 3. Variation of the most significant morphological measurements among species, *Microsternarchus javieri* n. sp. (N = 25), *Microsternarchus bilineatus* (N = 14), and *Microsternarchus brevis* (N = 9) tested with ANCOVA for species and covariate (body size). F- values are given. None of the interactions were significant. Significance levels: ** = p < 0.01. *** = p < 0.001. Ln = natural logarithm.

Variable	*M. javieri* n. sp., *M. bilineatus, M. brevis*		
	Species	Covariate (LEA)	Interaction
Ln maximum depth (D)	**19.41*****	139.26 ***	0.75
	M. javieri n. sp., *M. bilineatus*		
	Species	Covariate (HL)	Interaction
Ln eye diameter (ED)	**12.71****	12.98***	0.12
Ln internarinal distance (ID)	5.44*	33.30***	1.19
Ln interorbital distance (IO)	0.42	19.82***	0.70
Ln snout to posterior naris (SN)	2.55	39.23***	3.51
		(LEA)	
Ln caudal filament depth (CD)	0.0002	21.64***	0.00

previously-identified lineage C were distributed along the Anavilhanas archipelago in the lower to the mid portion of the Negro River, and in the lower Branco River basin. Morphologically, differences are subtle and challenging to establish with the naked eye in the field. However, there is a set of measurements that, when combined, separate *M. javieri* n. sp. from the other *Microsternarchus* species.

The average sequence distance (K2P) of 0% to 2.18%, and inter-specific distances of 17 to 24% coincide with the known increase in average COI distance with taxonomic rank (Hebert *et al.* 2003 a,b). Average intra-specific genetic distances of 0.13% and inter-specific genetic distances of 11.55% were reported among Amazonian fishes (Santana et al. 2023), and of 0.42% and 13.9%, respectively, among fishes from the east and west coast of India (Sadurudeen et al. 2017). The tendency also exists in other taxonomic groups, as intra-specific genetic distances of 0.43% and inter-specific genetic distances of 7.93% were reported for North American birds, and were considered sufficient to delimit species (Hebert et al. 2004). Therefore, our results fall within the ranges reported for other species, as the genetic differences between *Microsternarchus* species were far higher than differences within individuals, corroborating the hypothesis that *Microsternarchus javieri* n. sp. is a distinct biological species.

To reach inter-specific genetic differences as high as those shown here, considerable barriers must exist to prevent genetic flow between the two species (Leray et al. 2010; Hubert et al. 2012; Sadurudeen et al. 2017). However, there are no physical barriers between the lower, mid, and upper portions of the Negro River. *M. brevis* occurs from the middle portion of the Negro River basin upwards, whereas *M. javieri* n. sp. occurs from the middle portion downwards. We found the two species co-existing in only one location (Igarapé Quimicuri, 0º40'14.9" S, 63º16'3.6" W), where a single *M. javieri* n. sp. was captured among the dozens of streams explored. Certainly, it would be interesting to further explore the phylogeographic determinants that lead to the current distribution pattern of the two species.

We also demonstrated that the EOD of *M. javieri* n. sp. is different from that of *Microsternarchus brevis*. It would not be apparent from just looking at their pulses during the non-reproductive season, as differences seem to become more conspicuous during the later stages of gonadal maturation. The repetition rate recorded at rest for *M. javieri* n. sp. is higher than for *M. brevis's*, and the difference between the second and first phase areas produces the greater (negative) polarity balance in *M. javieri* n. sp. Such differences in EOD parameters can be important in species recognition and in signaling sexual identity, sexual maturity, and motivational state (Zakon 2002; Albert and Crampton 2005). Considering that the EODs are easily distinguishable only after laboratory analyses, it raises the question of how or if the sensory systems of the two species can distinguish both discharges in the wild where they occur in sympatry.

We also found sexual dimorphism in the EOD pulse of *M. javieri* n. sp., which differed between males and females in the repetition rate, power peak frequency, amplitude and duration of the second phase. Sexually dimorphic EODs are common across gymnotiforms such as *Sternopygus macrurus* Bloch and Schneider, 1801(Hopkins 1972), *Apteronotus leptorhynchus* Ellis, 1912 (Dulka and Maler 1994), *Eigenmannia virescens* Valenciennes, 1836 (Dunlap and Zakon 1998), *Brachyhypopomus pinnicaudatus* Hopkins, 1991 (Franchina and Stoddard 1998), *B. beebei* Schultz, 1944 (Stoddard 1999), and *Sternachogiton nattereri* Steindachner, 1868 (Cox Fernandes et al. 2010). These differences in EOD waveform are known to be crucial in sexual recognition and sexual selection (Stoddard 2006; Crampton et al. 2011). It has been postulated that DC electric fields in the water, such as the those produced by a negative polarity balance in the male EOD, can affect the ampullary electroreceptors of the females, which can have an indirect pathway to the pituitary, a gland that plays a crucial role in spawning (Heiligenberg et al. 1991). Therefore, the expansion of the negative phase in pulse-type fish might facilitate the reproductive success of these fish in their environment.

CONCLUSIONS

In this study we used an integrative taxonomic framework to describe a new species, *M. javieri* n. sp., within the tribe Microsternarchini. With our description here, the genus *Microsternarchus* now comprises five species: *M. bilineatus* Fernández-Yépez 1968, *M. brevis* Cox Fernandes, Nogueira, Williston, Alves-Gomes 2015, *M. longicaudatus* Sousa, Wosiacki, Muriel-Cunha, Prudente, Sousa, Peixoto 2024, *M. schonmanni* Cox Fernandes, Keeffe, Escamilla Pinilla 2024, and *M. javieri* Cox Fernandes, Escamilla Pinilla, Alves-Gomes 2025

Comparative material examined : For comparison of the new species with its closest congeners, the following museum specimens were examined: *Microsternarchus bilineatus*: VENEZUELA. San Bartolo River, Morichal Charcote, Guaricó, INHS 34027, 13; INHS 111262, 1.

Microsternarchus brevis: BRAZIL. Igarapé Quimicuri, Negro River basin, Amazonas, INPA-ICT 28585, 1; MCZ 171664, 1; INPA-ICT 42261, 2; ANSP 198325, 1; and INPA-ICT 42262, 3. Igarapé Curicuriari, Negro River basin, Amazonas, INPA-ICT 42267, 1.

ACKNOWLEDGMENTS

Special thanks to L. Rapp Py-Daniel at fish collection of the Instituto Nacional de Pesquisas da Amazônia (INPA) and Mark H. Sabaj, at the Academy of Natural Sciences of Drexel University (ANSP). We are grateful for the thoughtful comments from John P. Sullivan and an anonymous reviewer. We thank Jeff Podos, at University of Massachussetts (Umass, Amherst), Amherst for his helpful review on the language and comments, and David Matthews at UMass, Amherst, for taking Figure 6 fish images. Andrew Williston provided support with the CT Scan image taken at the Museum of Comparative Zoology (MCZ), at Harvard University. The fieldwork in the Rio Negro and Rio Branco, and the research associated with this work was supported by Conselho Nacional de Desenvolvimento Científico e Tecnológico (CNPq), Fundação de Amparo à Pesquisa do Estado do Amazonas (FAPEAM – Edital 002/2018) and INPA to JAG and CCF. A graduate scholarship and fieldwork resources were provided by CNPq, FAPEAM and Coordenação de Aperfeiçoamento de Pessoal de Nível Superior (CAPES) to CEP. This research was developed at INPA and UMass, Amherst. UMass Amherst, Natural History Collections provided support for CCF. Many thanks to field assistants of the Laboratório de Fisiologia Comportamental e Evolução (LFCE) at INPA.

REFERENCES

Albert, J. 2001. Species diversity and phylogenetic systematics of American knifefishes (Gymnotiformes, Teleostei). *Miscelaneous Publications: Museum of Zoology* 190: 1–127.

Albert, J.S.; Crampton, W.G.R. 2005. Diversity and phylogeny of Neotropical electric fishes. In: Bullock, T.H.; Hopkins, C.D.; Popper, A.N.; Fay, R.R. (Eds.). *Electroreception*. Springer, New York, p.360–409.

Alho, C.; Reis, R.; Aquino, P. 2015. Amazonian freshwater habitats experiencing environmental and socioeconomic threats affecting subsistence fisheries. *AMBIO* 44: 412–425.

Cox Fernandes, C.; Smith, T.G.; Podos, J.; Nogueira, A.; Inoue, L.; Akama, A.; et al. 2010. Hormonal and behavioral correlates of morphological variation in an Amazonian electric fish (*Sternarchogiton natteri*: Apteronotidae). *Hormones and Behavior* 58: 660–668.

Cox Fernandes, C.; Nogueira, A.; Alves-Gomes J.A. 2014. *Procerusternarchus pixuna*, a new genus and species of electric knifefish (Gymnotiformes: Hypopomidae, Microsternarchini)

from the Negro River, South America. *Proceedings of the Academy of Natural Sciences of Philadelphia* 163: 95–118.

Cox Fernandes, C.; Nogueira, A.; Williston, A.; Alves-Gomes JA. 2015. A new species of electric knifefish from the rio Negro, Amazon basin (Gymnotiformes: Hypopomidae, Microsternarchini). *Proceedings of the Academy of Natural Sciences of Philadelphia* 164: 213–227.

Cox Fernandes, C.; Williston, A. 2017. Redescription of *Microsternarchus bilineatus* (Fernandéz-Yépez, 1968) (Gymnotiformes: Hypopomidae, Microsternarchini), with the designation of a neo-type. *Proceedings of the Academy of Natural Sciences of Philadelphia* 165: 65–75.

Cox Fernandes, C.; Keeffe, R.M.; Escamilla Pinilla, C. 2024. *Microsternarchus schonmanni*, a new species of weakly electric fish (Gymnotiformes: Hypopomidae, Microsternarchini) from the Mamoré-Guaporé River Basin, Amazonas, Brazil. *Proceedings of the Academy of Natural Sciences of Philadelphia* 168: 237–249.

Crampton, W.G.R.; Lovejoy, N.R.; Waddell, J.C. 2011. Reproductive character displacement and signal ontogeny in a sympatric assemblage of electric fish. *Evolution* 65: 1650–1666.

Dagosta C.P.; de Pinna M. 2019. The fishes of the Amazon: Distribution and biogeographical patterns, with a comprehensive list of species. *Bulletin of the American Museum of Natural History* 431: 1–163.

Dingerkus, G.; Uhler, L.D. 1977. Enzyme clearing of Alcian blue stained whole small vertebrates for demonstration of cartilage. *Journal of Stain Technology* 52: 229–232.

Dulka, J.G.; Maler, L. 1994. Testosterone modulates chirping behavior in the weakly electric fish, *Apteronotus leptorhynchus*. *Journal of Comparative Physiology A* 174: 331–343.

Dunlap, K.D.; Zakon, H.H. 1998. Behavioral actions of androgens and androgen receptor expression in the electrocommunication system of an electric fish, *Eigenmannia virescens*. *Hormones and Behavior* 34: 30–38.

Franchina, C.R.; Stoddard, P.K. 1998. Plasticity of the electric organ discharge waveform of the electric fish *Brachyhypopomus pinnicaudatus*: Quantification of day-night changes. *Journal of Comparative Physiology A* 183: 759–768.

Hebert, P.D.N.; Cywinska, A.; Ball, S.L.; de Waard, J.R. 2003a. Biological identifications through DNA barcodes. *Proceedings of the Royal Society of London Biological Sciences* 270: 313–321.

Hebert, P.D.N.; Ratnasingham, S.; de Waard, J.R. 2003b. Barcoding animal life: Cytochrome c oxidase subunit 1 divergences among closely related species. *Proceedings of the Royal Society of London Biological Sciences* 270: S596–S599.

Hebert, P.D.N.; Stoeckle, M.Y.; Zemlak, T.S.; Francis, C.M. 2004. Identification of birds through DNA barcodes. *PLoS Biology* 2(10): e312.

Heiligenberg, W.; Rose, G. 1985a. Neural correlates of the jamming avoidance response (JAR) in the weakly electric fish *Eigenmannia*. *Trends in Neurosciences* 8: 442–449.

Heiligenberg, W.; Rose, G. 1985b. Phase and amplitude computations in the midbrain of an electric fish: intracellular studies of neurons participating in the jamming avoidance response of *Eigenmannia*. *The Journal of Neuroscience* 5: 515-531.

Heiligenberg, W.; Keller, C.H.; Metzner, W.; et al. 1991. Structure and function of neurons in the complex of the nucleus electrosensorius of the gymnotiform fish *Eigenmannia*: Detection and processing of electric signals in social communication. *Journal of Comparative Physiology A* 169: 151–164.

Hilton, E.J.; Cox Fernandes, C.; Sullivan, J.P.; Lundberg, J.G.; Campos-da-Paz, R. 2007. Redescription of *Orthosternarchus tamandua* (Boulenger, 1898) (Gymnotiformes, Apteronotidae), with reviews of its ecology, electric organ discharges, external morphology, osteology, and phylogenetic affinities. *Proceedings of the Academy of Natural Sciences of Philadelphia* 156: 1–25.

Hopkins, C.D. 1972. Sex differences in electric signaling in an electric fish. *Science* 176: 1035–1037.

Hopkins, C.D.; Comfort N.C.; Bastian J.; Bass A.H. 1990. Functional analysis of sexual dimorphism in an electric fish, *Hypopomus pinnicaudatus*, order Gymnotiformes. *Brain Behavioral Evolution* 35: 350–367.

Hubert, N.; Meyer, C.P.; Bruggemann, H.J.; Guérin, F.; Komeno, R.J.L et al. 2012. Cryptic diversity in Indo-Pacific coral-reef fishes revealed by DNA-barcoding provides new support to the centre-of-overlap hypothesis. *PLoS One* 7: e28987.

Jesus S.I.; Ferreira M.; Garcia C.; Braga Ribeiro L.; Alves-Gomes J.A.; Feldberg, E. 2016. First cytogenetic description of *Microsternarchus bilineatus* (Gymnotiformes: Hypopomidae) from Negro River (Brazilian Amazon). *Zebrafish* 13: 571–577.

Junk W.J.; Piedade, M.T.F.; Schöngart, J. 2011. A classification of major naturally occurring Amazonian lowland wetlands. *Wetlands* 31: 623–640.

Latrubesse, E.M.; Franzinelli, E. 2005. The late Quaternary evolution of the Negro River, Amazon, Brazil: Implications for island and floodplain formation in large unbranching tropical systems. *Geomorphology* 70: 372–397.

Leino, R.L; Jensen, K.M.; Ankley, G.T. 2005. Gonadal histology and characteristic histopathology associated with endocrine disruption in the adult fathead minnow (*Pimephales promelas*). *Environmental Toxicology and Pharmacology* 19: 85–89.

Leray, M.; Beldad, R.; Holbrook, S.J.; Schmitt R.J.; Planes, S.; Bernardi, G. 2010. Allopatric divergence and speciation in coral reef fish: the three-spot *Dascyllus, Dascyllus trimaculatus*, species complex. *Evolution* 64: 1218-1230.

Logan, M. 2010. Analysis of covariance (ANCOVA). In: Logan, M. (Eds.). *Biostatistical Design and Analysis Using R: A Practical Guide*. Wiley-Blackwell, West Sussex, p.448–457.

Mago-Leccia, F. 1994. *Electric Fishes of the Continental Waters of America*. Fundacion para el Desarrollo de las Ciencias Fisicas, Matematicas y Naturales (FUDECI), Caracas, 206p.

Maia, C.R.; Alves-Gomes, J.A. 2012. Utilização do código de barras de DNA na estimativa da diversidade de peixes elétricos do gênero *Microsternarchus* (Ostariophysi: Gymnotiformes) na bacia do Rio Negro, Amazonas. In: Souza, L.A.G.; Castellón, E.G. (Eds.). *Projeto Fronteira - Desvendando as Fronteiras do Conhecimento na Região Amazônica do Alto Rio Negro*. Editora INPA, Manaus, p.185–201.

Moraes, R.M.; Correa, S.B.; Doria, C.R.C.; Duponchelle, F.; Miranda, G.; Montoya, M.; et al. 2021. Biodiversity and ecological functioning in the Amazon. In: Nobre, C.; Encalada,

A.; Anderson, E.; Roca Alcazar, F.H.; Bustamante, M.; Mena, C.; et al. (Eds.). *Amazon Assessment Report*, Chapter 4. United Nations Sustainable Development Solutions Network, in New York, p. 4.1 - 4.33.

Nogueira, A. 2011. Diversidade específica em *Microsternarchus* (Gymnotiformes: Hypopomidae) da bacia do rio Negro e comportamento agonístico em cativeiro de uma nova espécie do gênero. Doctoral thesis, Instituto Nacional de Pesquisas da Amazônia (INPA), Brazil, 131p. (https://repositorio.inpa.gov.br/handle/1/37480). Acessed on 15 Jan 2024.

Sabaj, M.H. 2020. Codes for natural history collections in ichthyology and herpetology. *Copeia* 108: 593–669.

Sadurudeen, N.; Pavan-Kumar, A.; Gireesh-Babu, P.; Jaiswar, A.K.; Chaudhari, A.; Krishna, G.; et al. 2017. DNA barcoding of selected Perciformes (Infra Class: Teleostei) fishes from Indian coast. *Indian Journal of Biotechnology* 16: 315–321.

Santana, P.; Martins, T.; Lutz, Í.; Miranda, J.; da Silva, R.; Mesquita, D.; et al. 2023. DNA barcode reveals occurrence of threatened species and hidden diversity on Teleost fish trade in the Coastal Amazon. *Science Reports* 13: 19749.

Sousa, T.; Wosiacki, W.B.; Muriel-Cunha, J.; Prudente, B.S.; Sousa, R.S.; Peixoto, L.A.W. 2024. A new species of the electric fish *Microsternarchus* Fernández-Yépez 1968 (Gymnotiformes: Hypopomidae) from the lower Amazon basin, Brazil. *Zootaxa* 5448: 508–518.

Stoddard, P.K. 1999. Predation enhances complexity in the evolution of electric fish signals. *Nature* 400: 254–256.

Stoddard, P.K. 2006. Plasticity of the electric organ discharge waveform: contexts, mechanisms, and implications for electrocommunication. In: Ladich, F.; Collin, S.P.; Moller, P.; Kapoor, B.G. (Eds.). *Communication in Fishes,* v.2. NH Science, Enfield, p.623–646.

Sullivan, J. P. 1997. A phylogenetic study of the neotropical hypopomid electric fishes (Gymnotiformes: Rhamphichthyoidea). Ph. D. Dissertation, Duke University, Durham, 336 pp.

Tagliacollo, V.; Bernt, M.; Craig, J.; Oliveira, C.; Albert, J. 2016. Model-based total evidence phylogeny of Neotropical electric knifefishes (Teleostei, Gymnotiformes). *Molecular Phylogenetics and Evolution* 95: 20–33.

Zakon, H.H. 2002. Convergent evolution on the molecular level. *Brain Behavioral Evolution* 59: 250–261.

RECEIVED: 27/05/2024
ACCEPTED: 17/10/2024
ASSOCIATE EDITOR: Carlos David de Santana
DATA AVAILABILITY: The data that support the findings of this study are available, upon reasonable request, from the corresponding author [Carolina Escamilla Pinilla].

SUPPLEMENTARY MATERIAL

Escamilla Pinilla et al. Microsternarchus javieri, a new species of weakly electric fish (Gymnotiformes: Hypopomidae, Microsternarchini) from the Negro River basin, Amazonas, Brazil

Table S1. GenBank access codes of 17 hypopomids, 26 *M. brevis* and 27 *M. javieri* individuals selected for the genetic distance analysis.

Species	GenBank Access Code
Hypopygus neblinae	020278_CBX_N_{H._neblinae}
Hypopygus neblinae	020176_MAB_N_{H._neblinae}
Hypopygus neblinae	050003_QUI_N_{H._neblinae}
Akawaio penak	KF533335.1_Akawaio_penak_isolate_8795_{A._penak}
Akawaio penak	KF533336.1_Akawaio_penak_{A._penak}
Hypopomus artedi	GBOL1437-16|Hypopomus_artedi|COI-5P|MZ051479_{H._artedi}
Hypopomus artedi	GBOL1439-16|Hypopomus_artedi|COI-5P|MZ051261_{H._artedi}
Hypopomus artedi	GBOL3634-18|Hypopomus_artedi|COI-5P|MZ050946_{H._artedi}
Brachyhypopomus brevirostris	120187UBI_Brachy_brevirostris_{B._brevirostris}
Brachyhypopomus brevirostris	K2_Brachyhypopomus_brevirostris_{B._brevirostris}
Brachyhypopomus brevirostris	G3_Brachyhypopomus_brevirostris_{B._brevirostris}
Racenisia fimbriipinna	KF533337.1_Racenisia_fimbriipinna_{R._fimbriipinna}
Racenisia fimbriipinna	PQ356985_{R._fimbriipinna}
Racenisia fimbriipinna	PQ356986_{R._fimbriipinna}
Procerosternarchus pixuna	PQ356989_{P._pixuna}
Procerosternarchus pixuna	PQ356988_{P._pixuna}
Procerosternarchus pixuna	PQ356987_{P._pixuna}
Microsternarchus javieri	PQ356957_{M._javieri}
Microsternarchus javieri	PQ356932 _{M._javieri}
Microsternarchus javieri	11250NAI_{M._javieri}
Microsternarchus javieri	PQ356952_{M._javieri}
Microsternarchus javieri	PQ356953_{M._javieri}
Microsternarchus javieri	PQ356954_{M._javieri}
Microsternarchus javieri	PQ356934_{M._javieri}
Microsternarchus javieri	PQ356935_{M._javieri}
Microsternarchus javieri	PQ356936_{M._javieri}
Microsternarchus javieri	PQ356945_{M._javieri}
Microsternarchus javieri	PQ356945_{M._javieri}
Microsternarchus javieri	PQ356939_{M._javieri}
Microsternarchus javieri	PQ356941_{M._javieri}
Microsternarchus javieri	PQ356956_{M._javieri}
Microsternarchus javieri	PQ356937_{M._javieri}
Microsternarchus javieri	PQ356937_{M._javieri}
Microsternarchus javieri	PQ356946_{M._javieri}
Microsternarchus javieri	PQ356958_{M._javieri}
Microsternarchus javieri	PQ356938_{M._javieri}

Table S1. Continued

Species	GenBank Access Code
Microsternarchus javieri	PQ356951_{M._javieri}
Microsternarchus javieri	PQ356947_{M._javieri}
Microsternarchus javieri	PQ356948_{M._javieri}
Microsternarchus javieri	PQ35649_{M._javieri}
Microsternarchus javieri	PQ356950_{M._javieri}
Microsternarchus javieri	PQ356943_{M._javieri}
Microsternarchus javieri	PQ356942_{M._javieri}
Microsternarchus javieri	PQ356944_{M._javieri}
Microsternarchus brevis	PQ356965_{M._brevis}
Microsternarchus brevis	PQ356972_{M._brevis}
Microsternarchus brevis	PQ356973_{M._brevis}
Microsternarchus brevis	PQ356974_{M._brevis}
Microsternarchus brevis	PQ356975_{M._brevis}
Microsternarchus brevis	PQ356966_{M._brevis}
Microsternarchus brevis	PQ356976_{M._brevis}
Microsternarchus brevis	PQ356977_{M._brevis}
Microsternarchus brevis	PQ356980_{M._brevis}
Microsternarchus brevis	PQ356979_{M._brevis}
Microsternarchus brevis	PQ356978_{M._brevis}
Microsternarchus brevis	PQ356981_{M._brevis}
Microsternarchus brevis	PQ356984_{M._brevis}
Microsternarchus brevis	PQ356967_{M._brevis}
Microsternarchus brevis	PQ356982_{M._brevis}
Microsternarchus brevis	PQ356983_{M._brevis}
Microsternarchus brevis	PQ356968_{M._brevis}
Microsternarchus brevis	PQ356969_{M._brevis}
Microsternarchus brevis	PQ3560_{M._brevis}
Microsternarchus brevis	PQ356970_{M._brevis}
Microsternarchus brevis	PQ356964_{M._brevis}
Microsternarchus brevis	PQ356959_{M._brevis}
Microsternarchus brevis	PQ356961_{M._brevis}
Microsternarchus brevis	PQ356962_{M._brevis}
Microsternarchus brevis	PQ356963_{M._brevis}
Microsternarchus brevis	PQ356971_{M._brevis}

Table S2. Loading values from the first three Principal Components performed in *Microsternarchus javieri* (N = 25) and *Microsternarchus bilineatus* (N = 14) individuals using 18 morphological measurements.

Measurements	PC1	PC2	PC3
TL	0.26	0.12	0.11
LEA	0.26	0.10	0.14
H	0.25	0	-0.06
CL	0.24	0.13	0.16
SO	0.23	0.16	0.26
SA	0.24	0.18	0.05
CD	0.22	-0.16	-0.32
S	0.24	-0.18	-0.12
M	0.24	0.04	-0.16

Measurements	PC1	PC2	PC3
ED	0.21	0.41	-0.19
IO	0.22	0.04	-0.52
SV	0.25	0.09	0.03
SP	0.25	0.04	-0.14
D	0..21	-0.19	0.46
ID	0.20	-0.60	0.24
EO	0.24	0.08	0.10
SN	0.21	-0.51	-0.29
AF	0.25	0.08	0.18

Table S3. Electric organ discharge (EOD) parameters calculated for *Microsternarchus javieri*, (N = 27) and *Microsternarchus brevis* (N = 15) (Numbers in parentheses have negative values).

	***M. javieri* (N = 27)**		***M. brevis* (N = 15)**	
EOD Parameters	**Range**	**Mean ± SD**	**Range**	**Mean ± SD**
Mean inter-pulse intervals (ms)	7.96 – 22.02	13.35 ± 3.66	12.49 – 20.69	16.57 ± 2.28
Mean Repetition rate (Hz)	45.41 – 125.65	80.18 ± 20.95	48.32 – 80.03	61.43 ± 8.63
Coefficient of Variation	0.0013 – 0.0129	0.0038 ± 0.0025	0.0020 – 0.023	0.0069 ± 0.007
EOD duration/Silent phase duration ratio	0.29 – 2.01	1.06 ± 0.43	0.39 – 1.25	0.85 ± 0.24
Ratio amplitude Second/First phase	0.88 – 1.69	1.33 ± 0.22	0.85 – 1.59	1.17 ± 0.23
Polarity balance (%)	(36.72) – 14.79	(13.81) ± 12.90	(8.08) – 14.15	3.62 ± 6.53
Peak Power Frequency (KHz)	0.30 – 0.54	0.39 ± 0.06	0.34 – 0.41	0.37 - 0.02
First phase duration (%)	10.81 – 33.33	20.30 ± 5.87	11.73 – 30.88	17.91 ± 5.48
Second phase duration (%)	12.54 – 38.70	24.57 ± 7.98	12.44 – 32.66	19.41 ± 5.48
Third phase duration (%)	29.03 – 76.25	55.12 ± 12.66	41.66 – 75.19	62.67 ±10.26
First phase area (%)	25.27 – 56.09	35.42 ± 7.18	32.37 – 52.70	44.63 ± 6.48
Second phase area (%)	(68.36) – (42.60)	(56.90) ± 6.45	(54.04) – (42.9)	(48.18) ± 3.26
Third phase area (%)	1.29 – 20.31	7.67 ± 5.61	2.08 – 15.67	7.17 ± 3.8
Ratio area Second/First phase	0.75 – 2.39	1.68 ± 0.43	0.83 – 1.60	1.11 ± 0.24

Table S4. Electric organ discharge (EOD) parameters calculated for *Microsternarchus javieri* individuals (N=376) (Numbers in parentheses have negative values).

***M. javieri* (N= 376)**		
EOD Parameters	**Range**	**Mean ± SD**
Mean inter-pulse intervals (ms)	7.50-22.02	12.16 ± 2.59
Mean Repetition rate (Hz)	45.41-133.34	85.68 ± 16.92
Coefficient of Variation	0.0011-0.0350	0.0044 ± 0.0037
EOD duration/Silent phase duration ratio	0.30-2.56	1.02 ± 0.36
Ratio amplitude Second/First phase	0.38-2.18	1.15 ± 0.30
Polarity balance (%)	(35.91) - 44.92	(3.43) ± 17.02
Peak Power Frequency (KHz)	0.24-0.60	0.43 ± 0.06
First phase duration (%)	10.58-37.43	20.75 ± 4.43
Second phase duration (%)	12.34-48.93	23.38 ± 6.00
Third phase duration (%)	22.64-76.64	55.87 ± 7.77
First phase area (%)	25.18-69.47	42.17 ± 8.25
Second phase area (%)	(67.96) - (27.54)	(51.72) ± 8.51
Third phase area (%)	0.58-19.40	6.12 ± 2.80
Ratio area Second/First phase	0.41-2.53	1.31 - 0.44